Fast construction of the Kohn–Sham response function for molecules

Peter Koval[1], Dietrich Foerster[2] Olivier Coulaud[3]

February 11, 2010

[1] CNRS, HiePACS project, INRIA Sud-Ouest, 351 Cours de la Liberation, 33405, Talence, France
[2] CPMOH, Universite de Bordeaux 1, 351 Cours de la Liberation, 33405, Talence, France
[3] INRIA Bordeaux Sud-Ouest, HiePACS project, 351 Cours de la Liberation, 33405, Talence, France

Abstract

The use of the LCAO (Linear Combination of Atomic Orbitals) method for excited states involves products of orbitals that are known to be linearly dependent. We identify a basis in the space of orbital products that is local for orbitals of finite support and with a residual error that vanishes exponentially with its dimension. As an application of our previously reported technique we compute the Kohn–Sham density response function χ_0 for a molecule consisting of N atoms in $N^2 N_\omega$ operations, with N_ω the number of frequency points. We test our construction of χ_0 by computing molecular spectra directly from the equations of Petersilka–Gossmann–Gross in $N^2 N_\omega$ operations rather than from Casida's equations which takes N^3 operations. We consider the good agreement with previously calculated molecular spectra as a validation of our construction of χ_0. Ongoing work indicates that our method is well suited for the computation of the GW self-energy $\Sigma = \mathrm{i}GW$ and we expect it to be useful in the analysis of exitonic effects in molecules.

Accepted for publication in **Physica Status Solidi**, 05.02.2009 both as contribution to the Proceedings of TNT2009 conference (Barcelona, Spain) and as a featured article.

1 Introduction

The method of "linear combination of atomic orbitals" (LCAO) goes back to the early days of quantum mechanics [1] and remains a good choice in ab-initio calculations of molecules or solids. LCAO provides a parsimonious basis for representing molecular orbitals and one-particle Green's functions. However, electronic structure theory also involves the electronic density and the expression for the electronic density contains all non vanishing products of orbitals, a set of quantities that are known to be linearly dependent.

The many existing constructions of a basis in the space of products may be divided into two classes. A first type of construction, called "resolution of identity" method was proposed by Boys and Shavitt [2] and focuses on the representation of the electronic interaction, see also Casida [3]. For Slater-type functions a "density fitting" procedure was developed by Baerends *et al* [4, 5]. The goal of both of these methods is to represent the electronic density (a two-center quantity within LCAO method) in a basis of one-center functions. For a good discussion of these techniques, see [6].

A second class of methods provides a basis for both response functions and interactions. For solids and within the muffin-tin approach, a "product basis" was proposed by Aryasetiawan and Gunnarsson [7] who removed the linear dependence by orthogonalizing an overlap matrix. Gaussian-type auxiliary functions were also used in solid state theory [8]. Blase and Ordejón [9] used Gram-Schmidt orthogonalization to eliminate the linear dependence from products on the same atom.

Our own construction [10, 11] belongs to the second class of methods. It was developed in the context of LCAO for orbitals of finite support and keeps the locality properties of the underlying atomic orbitals. In the present paper we further test our calculational framework by computing spectra of medium sized molecules and we also give an expression of the GW self-energy in our product basis.

This paper is organized as follows. In the next section, we describe our construction of a basis in the space of products in terms of "dominant products". A construction of the Kohn–Sham response function is described in section

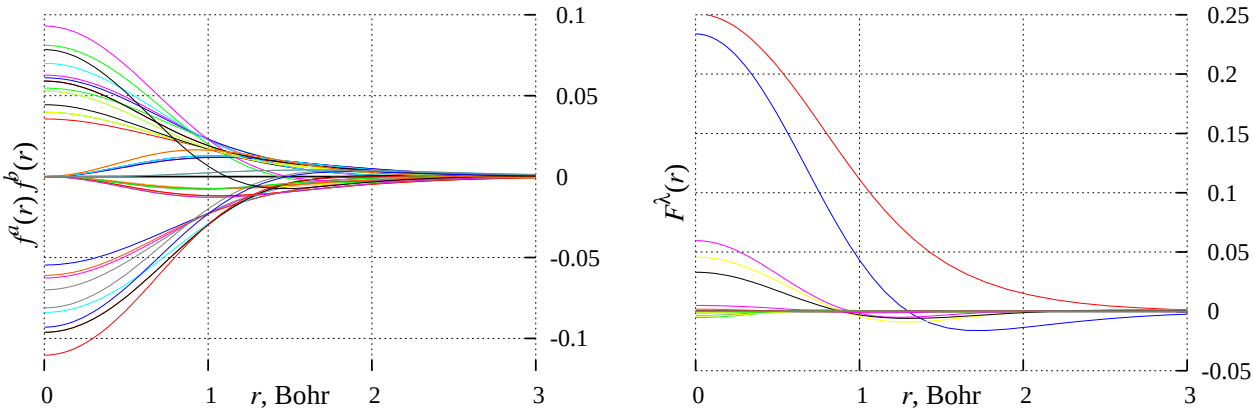

Figure 1: On the left panel, the orbital products (of total azimuthal angular momentum $m_z = 0$) are shown along the line connecting two (carbon) atoms. On the right panel, the corresponding dominant products are shown. The origin of x-axis is the middle point between atoms (on both panels). The linear dependence of the original orbital products and the small size of the dominant products basis are clearly visible.

3, and the application of this response function to the computation of molecular spectra is given in section 4. Finally, in section 5, we derive an expressions for the self-energy in Hedin's GW approximation in our basis and give our conclusions.

2 Reducing the number of orbital products

Restated in the succinct language of second quantization, the LCAO method consists of an expansion of the electron creation and annihilation operators $\psi^+(\boldsymbol{r},t)$, $\psi(\boldsymbol{r},t)$ in terms of electron operators $c_a(t)$ that belong to atomic orbitals

$$\psi^+(\boldsymbol{r},t) \sim \sum_a f^a(\boldsymbol{r}) c_a^+(t). \tag{1}$$

The functions $\{f^a(\boldsymbol{r})\}$ are atom centered orbitals, the operator $c_a^+(t)$ create localized electrons in these orbitals and the symbol $\sim$ alludes to the question of completeness of these LCAO orbitals, a difficulty we shall ignore in the following. Most molecular response functions involve the electronic density $n(\boldsymbol{r},t)$ and, therefore, the square of the previous expansion

$$n(\boldsymbol{r},t) = \psi^+(\boldsymbol{r},t)\psi(\boldsymbol{r},t) \sim \sum_{a,b} f^a(\boldsymbol{r}) f^b(\boldsymbol{r}) c_a^+(t) c_b(t).$$

It is well known in quantum chemistry that the products of orbitals $\{f^a(\boldsymbol{r})f^b(\boldsymbol{r})\}$ that parametrize this density are linearly dependent. A good illustration of this fact is provided [12] by the harmonic oscillator and its Hermite wave functions $\phi_n(x) = H_n(x)\mathrm{e}^{-x^2/2}$ where $\frac{N(N+1)}{2}$ products $\{\phi_m(x)\phi_n(x)\}_{m,n=1..N}$ span a space of only $2N+1$ dimensions. The set of products $\{f^a(\boldsymbol{r})f^b(\boldsymbol{r})\}$ is usually parametrized by extra auxiliary fitting functions [4, 5, 13]. In this paper, we use an alternative procedure that involves no fitting functions whatsoever [10]. We proceed in two steps:

- for each pair of atoms, the orbitals of which overlap, we enumerate all products $F^M(\boldsymbol{r}) = f^a(\boldsymbol{r})f^b(\boldsymbol{r})$,
- we compute their metric or matrix of overlaps G^{MN}, diagonalize this matrix and employ its eigenvectors and eigenvalues to define *dominant products* $F^\lambda(\boldsymbol{r})$

$$\begin{aligned} G^{MN} &= \int \frac{F^M(\boldsymbol{r})F^N(\boldsymbol{r}')}{|\boldsymbol{r}-\boldsymbol{r}'|}\,\mathrm{d}^3r\,\mathrm{d}^3r', \\ G^{MN}X_N^\lambda &= \lambda X_M;\ F^\lambda(\boldsymbol{r}) = X_M^\lambda F^M(\boldsymbol{r}). \end{aligned} \tag{2}$$

We use the Coulomb metric, the favorable properties of which are well known in quantum chemistry [14]. Although the procedure is carried out separately for each pair of atoms at a time, the overall result is a basis in the space of

all products. Our procedure provides us with (i) a set of dominant functions $\{F^\lambda(\boldsymbol{r})\}$ and (ii) their relation with the original products

$$f^a(\boldsymbol{r})f^b(\boldsymbol{r}) \sim \sum_{\lambda>\lambda_{\min}} V_\lambda^{ab} F^\lambda(\boldsymbol{r}). \tag{3}$$

Here we ignore the products that have a Coulomb norm less than $\lambda_{\min}$. The finite support of the original atomic orbitals and the locality of our construction are reflected in the sparse character of the "vertex" V_λ^{ab}.

Due to (i) the finite support of the original orbitals and (ii) the locality of our procedure, identifying the dominant functions in a molecule of N atoms takes asymptotically only $O(N)$ operations. Moreover, a very accurate representation of orbital products as an expansion about intermediate points of each pair is possible thanks to two powerful algorithms developed by Talman [15]. For the case of bilocal products, the results of our procedure are illustrated in figure 1.

For reasons not yet entirely understood [16], the eigenvalues of the metric (2) are asymptotically evenly spaced on a logarithmic scale, in formal analogy with the $1/f$ noise that occurs in electronics [17]. As a welcome consequence, the residual (asymptotic) error of our algorithm vanishes exponentially fast with the number of dominant products retained.

3 Computation of the Kohn–Sham density response in $O(N^2 N_\omega)$ operations

The usual LCAO method provides us with a tensor basis for the electron operators $c_a(t)$, $c_b^+(t')$ and for their Green's function $\mathrm{i}G_{ab}(t-t') = T\langle c_a(t)c_b^+(t')\rangle$. Similarly, our dominant products provide a tensor basis for the density

$$\begin{aligned} n(\boldsymbol{r},t) &= \psi^+(\boldsymbol{r},t)\psi(\boldsymbol{r},t) = \sum_\lambda n_\lambda(t)F^\lambda(\boldsymbol{r}) \\ \text{with}\quad n_\lambda(t) &= \sum_{a,b} c_a^+(t)V_\lambda^{ab}c_b(t). \end{aligned}$$

Recalling that the response function coincides with the density–density correlator [18, 19]

$$\chi_0(\boldsymbol{r},\boldsymbol{r}',t-t') = -\mathrm{i}\langle T\{n(\boldsymbol{r},t)n(\boldsymbol{r}',t')\}\rangle_{\text{connected}},$$

we obtain a representation of the response function

$$\chi_0(\boldsymbol{r},\boldsymbol{r}',t-t') \equiv \sum_\mu F^\mu(\boldsymbol{r})\chi^0_{\mu\nu}(t-t')F^\nu(\boldsymbol{r})$$

in terms of a time-dependent matrix $\chi^0_{\mu\nu}(t-t')$

$$\chi^0_{\mu\nu}(t-t') = -\mathrm{i}\langle T\{n_\mu(t)n_\nu(t')\}\rangle_{\text{connected}} = \mathrm{i}\sum_{a,b,c,d} V_\mu^{ba}G_{ac}(t-t')V_\nu^{cd}G_{db}(t'-t). \tag{4}$$

From figure 2 and from the locality of the vertex we see that for $N \gg 1$ atoms, the computation of $\chi^0_{\mu\nu}(t-t')$

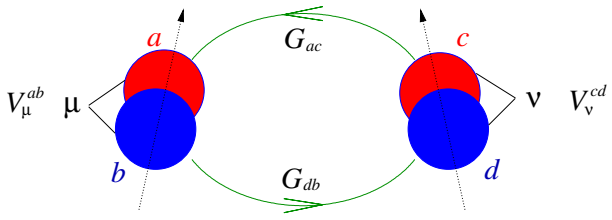

Figure 2: Particle–hole diagram for Kohn–Sham response in a basis of dominant products. The vertex V_μ^{ab} connects pairs of orbitals a, b to a dominant product μ. The propagators connect the orbitals within the atom quadruplet. For a given pair of dominant products (μ,ν), only the orbitals that belong to the corresponding atom quadruplet must be summed over. Therefore, the total computational effort scales as $O(N^2N_\omega)$.

takes $O(N^2)$ operations. More precisely, the number of operations is $O(N^2 N_\omega \log(N_\omega))$ for N_ω frequencies where the $N_\omega \log(N_\omega)$ factor is due to the use of fast Fourier techniques in evaluating equation (4).

To achieve a well controlled calculation, we express $\chi^0_{\mu\nu}(\omega)$ in terms of its spectral representation

$$\chi^0_{\mu\nu}(\omega) = \int_{-\infty}^{\infty} \mathrm{d}\lambda \frac{a_{\mu\nu}(\lambda)}{\omega - \lambda + \mathrm{i}\varepsilon}, \tag{5}$$

where $a_{\mu\nu}(\lambda)$ is a spectral function associated with response function $\chi^0_{\mu\nu}(\omega)$. We now indicate how expression (5) can be derived, for instance, by representing the Green's functions in equation (4) in terms of its spectral functions. We first recall the standard expression [18, 20] for Green's function in terms of molecular orbitals $\psi_E(\boldsymbol{r})$

$$G(\boldsymbol{r}, \boldsymbol{r}', t - t') = \mathrm{i}\theta(t' - t) \sum_{E<0} \psi_E(\boldsymbol{r})\psi_E(\boldsymbol{r}')\mathrm{e}^{-\mathrm{i}E(t-t')} - \mathrm{i}\theta(t - t') \sum_{E>0} \psi_E(\boldsymbol{r})\psi_E(\boldsymbol{r}')\mathrm{e}^{-\mathrm{i}E(t-t')}.$$

We then rewrite it using the LCAO expression for the molecular orbitals $\psi_E(\boldsymbol{r}) \equiv \sum_a X^E_a f^a(\boldsymbol{r})$ and introducing density matrices of particles $\rho^+_{ab}(s) = \sum_{E>0} X^E_a X^E_b \delta(s - E)$ and holes $\rho^-_{ab}(s) = \sum_{E<0} X^E_a X^E_b \delta(s - E)$

$$G_{ab}(t - t') = \mathrm{i}\theta(t - t') \int ds\ \rho^-_{ab}(s)\mathrm{e}^{-\mathrm{i}s(t'-t)} - \mathrm{i}\theta(t - t') \int ds\ \rho^+_{ab}(s)\mathrm{e}^{-\mathrm{i}s(t-t')}.$$

Inserting the last expression into equation (4), we identify the spectral function $a_{\mu\nu}(\lambda)$ in equation (5)

$$a_{\mu\nu}(\lambda) = \sum_{a,b,c,d} \left[V^{ba}_\mu \rho^+_{ac} \otimes V^{cd}_\nu \overline{\rho}^-_{db} \right](\lambda). \tag{6}$$

Here the overlined density $\overline{\rho}$ refers to a reflection of the argument $\overline{\rho}(x) = \rho(-x)$ and the notation $\otimes$ represents the convolution.

The convolutions in equation (6) can be done in $O(N_\omega \log(N_\omega))$ operations using the FFT technique, provided the density matrices $\rho^\pm_{ab}(s)$ are discretised on an uniform grid. The discretisation of stick-like density matrices is done with a simple algorithm—dividing the spectral weight between adjacent grid points according to the distance between an eigenenergy E and the grid point [11]. The integration over λ in equation (5) can also be represented as a convolution and may be computed in a fast manner using the FFT technique [11].

We checked our results against the exact but slow expression of the Kohn–Sham density response, i. e.

$$\chi_0^{\mathrm{exact}}(\boldsymbol{r}, \boldsymbol{r}', \omega) = \sum_{E,F} (n_F - n_E) \frac{\psi_E(\boldsymbol{r})\psi_F(\boldsymbol{r})\psi_E(\boldsymbol{r}')\psi_F(\boldsymbol{r}')}{\omega - (E - F) - \mathrm{i}\varepsilon(n_E - n_F)}$$

and its corresponding expression in our tensor basis (see figure 3 for a comparison between exact and fast results). This summarizes our method of constructing the Kohn–Sham density response function χ_0 in $O(N^2 N_\omega \log(N_\omega))$ operations. Next we will test our construction on molecular spectra.

4 Application of χ_0 to molecular spectra

The most direct application of χ_0 as constructed in the previous section is the computation of excitation spectra of molecules.

The excitation properties of molecules are determined by an interacting response function χ that is related to the non interacting response function χ_0 [22] via a Dyson type equation

$$\chi = \frac{\delta n}{\delta V_{\mathrm{ext}}} = \frac{1}{1 - f_{\mathrm{Hxc}}\chi_0}\chi_0. \tag{7}$$

The TDDFT kernel $f_{\mathrm{Hxc}} = \dfrac{\delta V_{\mathrm{Hxc}}}{\delta n}$ becomes a matrix in the basis of dominant products

$$f^{\mu\nu}_{\mathrm{Hxc}} = \iint \frac{F^\mu(\boldsymbol{r})F^\nu(\boldsymbol{r}')}{|\boldsymbol{r} - \boldsymbol{r}'|}\,\mathrm{d}^3r\mathrm{d}^3r' + \iint F^\mu(\boldsymbol{r})\frac{\delta V_{\mathrm{xc}}(\boldsymbol{r})}{\delta n(\boldsymbol{r}')}F^\nu(\boldsymbol{r}')\,\mathrm{d}^3r\mathrm{d}^3r'. \tag{8}$$

In this work, we focus on the local density approximation (LDA) for the exchange–correlation potential. In this case $f_{\mathrm{xc}}(\boldsymbol{r}, \boldsymbol{r}') = \frac{\mathrm{d}V_{\mathrm{xc}}(n)}{\mathrm{d}n}(\boldsymbol{r})\delta(\boldsymbol{r} - \boldsymbol{r}')$ and its matrix elements are local in coordinate space.

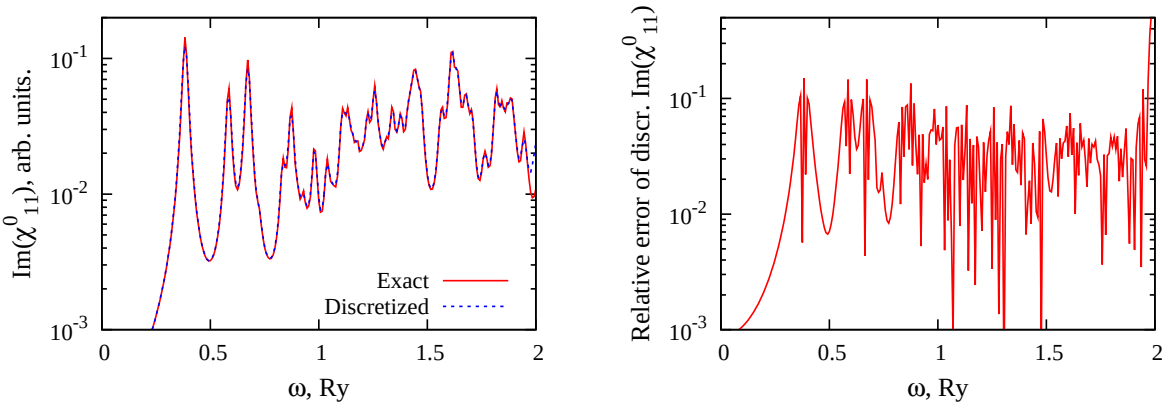

Figure 3: An element of the response function $\chi^0_{\mu\nu}$ of benzene. The Kohn–Sham eigenstates were generated using the SIESTA package [21] with default settings. The discretised response function is computed in the frequency window $\omega < \omega_{\max}$, $\omega_{\max} = 2$ Rydberg with $N_\omega = 512$ data points. ε is chosen to be $1.5\Delta\omega$, where the discretisation spacing is $\Delta\omega = 2\omega_{\max}/N_\omega$.

4.1 Calculation of the interaction kernel f_{Hxc}

In the construction of dominant products, we distinguish between (i) coincident and (ii) distinct or bilocal pairs of atoms. The former have full rotational symmetry, while the latter have only axial symmetry with respect to a line connecting their centers. Therefore the expansion of the bilocal products is done in an appropriately rotated coordinate frame. Both local and bilocal dominant products are expressed as a sum over angular–radial functions in a suitable coordinate system

$$F^\mu(\boldsymbol{r}) = \sum_l F^\mu_l(|\boldsymbol{r} - \boldsymbol{C}_\mu|) Y_{lm_\mu}(\boldsymbol{R}_\mu(\boldsymbol{r} - \boldsymbol{C}_\mu)), \tag{9}$$

where the rotation $\boldsymbol{R}_\mu$ and the shift $\boldsymbol{C}_\mu$ are determined by the atom pair. Using the theory of angular momentum, one can reduce the Coulomb interaction $\iint \frac{F^\mu(\boldsymbol{r})F^\nu(\boldsymbol{r}')}{|\boldsymbol{r}-\boldsymbol{r}'|}\,\mathrm{d}^3r\mathrm{d}^3r'$ to a sum over elementary two-center Coulomb integrals

$$(\boldsymbol{C}|\boldsymbol{C}') = \iint \frac{\mathrm{g}_{lm}(\boldsymbol{r} - \boldsymbol{C})\mathrm{g}_{l'm'}(\boldsymbol{r}' - \boldsymbol{C}')}{|\boldsymbol{r} - \boldsymbol{r}'|}\,\mathrm{d}^3r\mathrm{d}^3r' \tag{10}$$

between two functions of spherical symmetry $\mathrm{g}_{lm}(\boldsymbol{r})$. When the orbitals overlap, the Coulomb integrals are computed in the momentum space (where they become local) while, if they do not overlap, the Coulomb interaction is calculated exactly in terms of moments. For converting between coordinate and momentum space, we use Talman's fast Bessel transform [15].

Unlike the Hartree kernel, the LDA exchange–correlation kernel is local in coordinate space and a numerical integration is an appropriate procedure for it. The integrand $F^\mu(\boldsymbol{r})f_{\mathrm{xc}}(\boldsymbol{r})F^\nu(\boldsymbol{r})$ is of non trivial support due to the lens-shaped support of the dominant products. However, the non spherical part of this volume is small for neighboring atoms and we used spherical coordinates centered about a midpoint between the centers of the dominant products $F^\mu(\boldsymbol{r})$, $F^\nu(\boldsymbol{r})$. The integration is done with a Gauss–Legendre method along the radial coordinate and with a Lebedev quadrature [23] over the solid angle. A moderate number of integration points leads to a sufficient accuracy in the exchange–correlation matrix elements.

The computational complexity of the Hartree kernel $f^{\mu\nu}_{\mathrm{H}}$ and the exchange–correlation kernel $f^{\mu\nu}_{\mathrm{xc}}$ are $O(N^2)$ and $O(N)$, respectively. In practice, the calculation of the kernel f_{Hxc} is faster than the calculation of the non interacting response χ_0 by an order of magnitude.

4.2 An iterative method for finding the interacting polarizability

Expression (7) for the interacting response $\chi_{\mu\nu}$ involves matrix multiplications and inversion and this would appear to require $O(N^3N_\omega)$ operations, more than the $O(N^2N_\omega)$ complexity of the non interacting response $\chi^0_{\mu\nu}$. Fortunately,

the polarizability P is an average quantity[1]

$$P(\omega) = \sum_{\mu,\nu} d^\mu \chi_{\mu\nu}(\omega) d^\nu, \tag{11}$$

that is easy to compute using an iterative method of the Krylov type [11]. A biorthogonal Lanczos method [24] allows us to find a simple representation for the (non hermitian) matrix $A = 1 - f_{\rm Hxc}\chi^0$

$$A = \sum_{n,m} |L^n\rangle t_{nm} \langle R^m|, \tag{12}$$

where the matrix t_{nm} is tridiagonal. The set of vectors $|L^n\rangle$ and $\langle R^m|$ build up the identity in the Krylov space, $\langle R^m|L^n\rangle = \delta^{mn}$. Therefore, if we choose the starting vectors $|L^1\rangle$ and $\langle R^1|$ in the direction of the dipole moment d and of $\chi_0 d$, respectively

$$|L^1\rangle = d;\ \langle R^1| = \chi^0 d, \tag{13}$$

then the interacting polarizability takes a particularly simple form

$$P(\omega) = t_{11}^{-1} \langle d|\chi_0(\omega)|d\rangle. \tag{14}$$

Here, we multiply the Kohn–Sham (non interacting) polarizability with the first element of the inverse matrix t_{nm}.

The computational complexity of the iterative method is $O(N^2 N_{\rm K})$, where $N_{\rm K}$ is the dimension of the Krylov subspace. In our calculation $N_{\rm K}$ is very small compared to the number of dominant products and grows slowly as we increase the size of the system. In conclusion, our method requires a total of $O(N^2 N_\omega \log(N_\omega))$ operations to compute the molecular polarizability $P(\omega)$.

4.3 Memory requirements

The Kohn–Sham response matrix requires $O(N^2 N_\omega)$ memory. For instance, in the case of indigo dye, we need approximately 4 GBytes, where we have exploited the diagonal symmetry of the response matrix, using single precision complex numbers, and calculating for 256 frequencies. This is beyond the capacity of most contemporary desktop computers. The storage of the response matrix on a hard disk is not an option because the matrix is generated element by element for all frequencies at once, but needed (in the iterative computation of polarizability) as a frequency dependent matrix. For this reason, we have to employ parallel machines if a large molecule, say 100 atoms, is to be treated. Currently, we are implementing OpenMP and MPI parallelized versions of our algorithm.

4.4 Some illustrative results

We illustrate our method on benzene, indigo and fullerene C_{60}. Benzene serves as a test whether our basis represents the non interacting response function correctly. For indigo and fullerene, we compare our results with those of ADF [5] and Quantum Espresso [25], respectively.

In figure 4 we compare two theoretical calculations with experimental data [26] for benzene (C_6H_6). Both calculations make use of the iterative method of section 4.2 but we used (i) the basis of dominant products and (ii) the basis of products of (Kohn–Sham) eigenstates in these calculations. In the basis of products of eigenstates, the non interacting response χ_0 is a diagonal matrix [27] of size $N_{\rm occ}N_{\rm virt} \sim N^2$, that is easy to compute. Therefore, the comparison (i) vs (ii) allows us to assess whether there are enough dominant products for representing the Kohn–Sham response function. The size of the set of products of molecular orbitals grows as N^2 and the TDDFT kernel becomes a dense matrix, leading to an overall complexity scaling $O(N^3 N_\omega)$ and limiting the possibility of such a comparison to relatively small molecules like benzene or naphthalene. The basis is chosen to contain 1238 dominant products, which is considerable less than the 108*109/2=5886 original products.

The good agreement of the two theoretical calculations indicates the validity of our method as a whole and the adequacy of the dominant product's basis for representing the Kohn–Sham response function.

By comparison with experiment, the collective peak is slightly blue-shifted. There are several reasons for this discrepancy. A first reason is the limited applicability of the simple LDA functionals — we use the Perdew–Zunger LDA functional, which is the default functional in the SIESTA package [21]. A preliminary calculation with a GGA

[1] In this equation and below, we focus on the calculation of a particular component of the polarizability tensor and remove tensor indices from the polarizability $P(\omega)$ and Cartesian vector indices from the dipole momenta $d_i^\mu = \int F^\mu(\boldsymbol{r})\boldsymbol{r}_i\,{\rm d}r$. However, a corresponding block-Lanczos algorithm exists and allows for a faster simultaneous calculation of all components of the polarizability tensor [11].

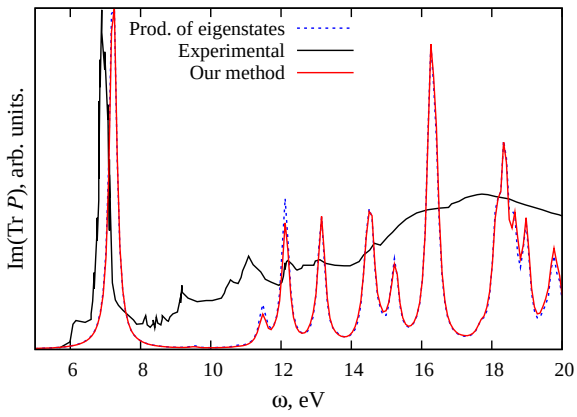

Figure 4: The interacting polarizability of benzene computed with two iterative methods compared with the experimental spectrum of benzene. The calculations differ by their basis – dominant products versus products of eigenstates. The input of both calculations is generated in a SIESTA run. Although different types of product basis are employed, the agreement between the theoretical results is good. The experimental spectrum shows a slightly red-shifted collective peak. See the text for a discussion of possible reasons of this discrepancy.

functional shows better results. A second reason is the incompleteness of the LCAO basis set — we employed a double-zeta polarized (DZP) basis which is the default basis in the SIESTA package. A third reason is our choice of the pseudo potential. We have been using the pseudo potentials published on the SIESTA Internet site [28] (LDA potentials of Troullier-Martins type adapted from ABINIT package [29]). Surely one can perform a fine tuning of the parameters, but this is beyond the scope of this paper. Therefore, the remaining calculations presented below are done with the same set of parameters.

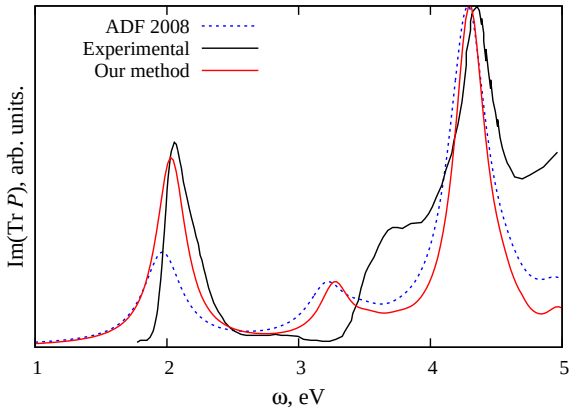

Figure 5: Comparison of the absorption of indigo dye computed with the ADF package versus our method. DFT calculations are done independently in ADF and SIESTA. Nevertheless, theoretical spectra agree except for a factor of 2 in the height of the HOMO–LUMO peak. In the range between 3–4 eV experiment and theory differ. The deviation might be caused by the presence of solvent in experimental setup.

In figure 5 we compare two theoretical calculations with experimental data [32] for the indigo dye ($C_{16}N_2O_2H_{10}$). The first calculation is done within the ADF package [5] with parameters similar to SIESTA's default parameters, while the second calculation is done with our method (details of the calculation are collected above in the discussion of results for benzene).

Both calculations agree except for the strength of the HOMO–LUMO transition. The experimental spectrum is in overall agreement with both calculations: three resonances are seen, while the middle resonance is probably disturbed by the presence of the solvent.

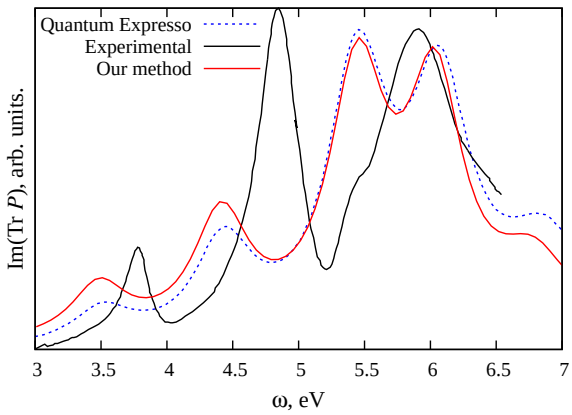

Figure 6: Theory versus experiment for absorption of fullerene C_{60}. Experimental data are from [30] and we compare our result with those of [31]. The theoretical results agree with each other and disagree with experiment. This might indicate an inadequacy of the LDA exchange–correlation functional for large molecules or be due to the presence of a solvent in the experimental setup. Excitonic effects may be another reason for this discrepancy.

We kept about 2100 dominant products and 256 frequency points in this calculation. The current implementation took 3.5 hours, if run on one thread, on an Intel Xeon processor at 2.50 GHz.

In figure 6 we compare theoretical and experimental spectra for fullerene C_{60}. The calculation by Rocca *et al* [31] agrees remarkably well with our calculation, while the experimental results [30] are blue-shifted compared with theory (details of the calculation are collected above in the discussion of results for benzene).

The disagreement might be due to use of the LDA functional. A solvent usually gives rise to a uniform red shift of experimental data [33] which is not the case in this example. We believe that excitonic effects cause the discrepancy in this large molecule.

We kept about 8700 dominant products and used 128 frequency points. The current implementation requires 18.4 hours, if run on one thread, on an Intel Xeon processor at 2.50 GHz.

The agreement between our calculations with those done by other authors and with experiment validates our construction of a basis in the space of products and our construction of the Kohn–Sham response function χ_0.

5 Hedin's GW self-energy in the product basis

It is known that particle–hole interactions in organic semiconductors cannot be described adequately by TDDFT. Such systems, however, can be modelled by Hedin's GW approximation [34, 35].

Let us show how to express Hedin's GW self-energy [36] in terms of our concepts $\{F^\lambda(\boldsymbol{r}), V^{ab}_\lambda\}$. Although the self-energy operator Σ should, in principle, be determined self-consistently using Hedin's set of integral equations, even a "one shot" approximation to the self-energy has been shown to improve the quasi particle energies compared to TDDFT energies. The self energy is given by [36, 37]

$$\Sigma(\boldsymbol{r},\boldsymbol{r}',t-t') = \mathrm{i}G_0(\boldsymbol{r},\boldsymbol{r}',t-t')W(\boldsymbol{r},\boldsymbol{r}',t-t'), \tag{15}$$

where $W = \frac{1}{1-f_{\mathrm{H}}\chi_0} f_{\mathrm{H}}$ is a RPA-screened Coulomb interaction that makes use of the non interacting KS response χ_0 and G_0 is the non interacting Green's function. To see the form this equation takes in our basis of dominant functions, we define a self energy matrix and expand the Greens function G_0

$$\begin{aligned} \Sigma^{ab}(t-t') &= \int \mathrm{d}^3r\mathrm{d}^3r' f^a(\boldsymbol{r})\Sigma(\boldsymbol{r},\boldsymbol{r}',t-t')f^b(\boldsymbol{r}') \\ G_0(\boldsymbol{r},\boldsymbol{r}',t-t') &= \sum_{a,b} G^0_{ab}(t-t')f^a(\boldsymbol{r})f^b(\boldsymbol{r}'). \end{aligned}$$

Inserting $\Sigma = \mathrm{i}G_0W$ and using the representation of products (3) we find the following tensor form of the GW

approximation

$$\Sigma^{ab}(t-t') = \mathrm{i} \sum_{\mu,\nu,a',b'} V_\mu^{aa'} V_\nu^{bb'} G^0_{a'b'}(t-t') W^{\mu\nu}(t-t'),$$

$$W^{\mu\nu}(t-t') \quad = \quad \int \mathrm{d}^3 r \mathrm{d}^3 r' \, F^\mu(\boldsymbol{r}) W(\boldsymbol{r},\boldsymbol{r}',t-t') F^\nu(\boldsymbol{r}').$$

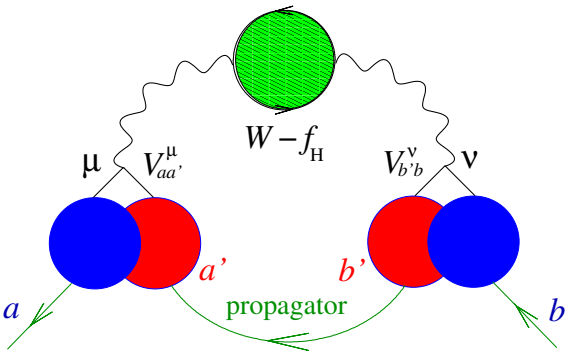

Figure 7: Diagram for the self-energy Σ in a "one shot" GW approximation. The vertices $V_\mu^{aa'}$ and $V_\nu^{b'b}$ are sparse – only the orbitals and products belonging to a given quadruplet of atoms contribute to the trace. Therefore, the computational effort for self energy Σ scales as $O(N^2 N_\omega)$ once the screened Coulomb interaction is known.

The direct computation of the screened Coulomb interaction $W^{\mu\nu}$ requires *a priori* $O(N^3 N_\omega)$ operations while the rest of the calculation of Σ^{ab} scales as $O(N^2 N_\omega)$. This is due to the locality of the vertex V_μ^{ab} (see the diagrammatic representation of the self-energy in figure 7). The situation here is similar as in the calculation of $\chi^0_{\mu\nu}$.

6 Conclusions

In this paper we reviewed our extension of the LCAO method to densities and excited states and we gave first applications of this method. One application is a convenient construction of the non interacting Kohn–Sham response in $O(N^2 N_\omega)$ operations. Another application is the use of this response function to compute electronic excitation spectra within TDDFT linear response, again in $O(N^2 N_\omega)$ operations. We illustrated our method of computing spectra using benzene, indigo and fullerene and we also confirmed the $O(N^2 N_\omega)$ complexity scaling of our method. A drawback of our construction of χ_0 is its high memory requirement— one could use a MPI parallelization to address this problem. We also mentioned that our method is suitable for application to the GW approximation which we cast in an appropriate tensor form.

Because our method provides (i) a simple basis for the electronic density and (ii) the Kohn–Sham response function we believe it will be useful in treating excitonic effects in molecular physics.

Acknowledgement

It is our pleasure to thank James Talman (University of Western Ontario, London) for contributing two crucial algorithms to this project, for making unpublished computer codes of these algorithms available to us, for many fruitful discussions and for useful correspondence.

D.F. is grateful to Peter Fulde for extensive and continued support and for inspiring visits at MPIPKS, Dresden that provided perspective for the present work. Part of the collaboration with James Talman was done in the pleasant environment of MPIPKS. D.F. acknowledges the kind hospitality extended to him by Gianaurelio Cuniberti at the Nanophysics Center of Dresden.

Both of us are indebted to Daniel Sánchez-Portal (DIPC, Donostia) for strong support of this project and for advice and help on the SIESTA code. We also thank Andrei Postnikov (Paul Verlaine University, Metz) for useful advice.

Ross Brown (IPREM, Pau) helped with experimental data on indigo dye and discussions. We acknowledge useful advice by Isabelle Baraille (IPREM, Pau), Nguyen Ky and Pierre Gay (DRIMM, Bordeaux), and Alain Marbeuf (CPMOH, Bordeaux).

We thank Mark E. Casida and Bhaarathi Natarajan (Joseph Fourier University, Grenoble) and their colleagues at Centro de Investigacion, Mexico for letting us use their deMon2k code and for much help with it. Stan van Gisbergen's (Vrije Universiteit, Amsterdam) provided us with a trial license of ADF and gave us useful comments on the algorithms implemented in ADF.

This work was financed by the French ANR project "NOSSI" (Nouveaux Outils pour la Simulation de Solides et Interfaces). Financial support and encouragement by "Groupement de Recherche GdR-DFT++" is gratefully acknowledged.

References

[1] R. S. Mulliken's Nobel Lecture, Science **157**, 13 (1967).

[2] S. F. Boys, I. Shavitt., University of Wisconsin Naval Research Laboratory Report WIS-AF-13 (1959).

[3] M. E. Casida, in *Recent Advances in Density Functional Theory*, edited by D. P. Chong (World Scientific, Singapore, 1995), p. 155.

[4] E. J. Baerends, D. E. Ellis, P. Ros, Chem. Phys. **2**, 41 (1973).

[5] G. Te Velde, F. M. Bickelhaupt, E. J. Baerends, C. Fonseca Guerra, S. J. A. van Gisbergen, J. G. Snijders, T. Ziegler, J. Comput. Chem. **22**, 931 (2001); S. J. A. van Gisbergen, C. Fonseca Guerra, E. J. Baerends, J. Comput. Chem. **21**, 1511 (2000).

[6] C.-K. Skylaris, L. Gagliardi, N. C. Handy, A. G. Ioannou, S. Spencer, A. Willetts, J. Mol. Struct. THEOCHEM **501–502**, 229 (2000).

[7] F. Aryasetiawan and O. Gunnarsson, Phys. Rev. **B 49**, 16214 (1994); A. Stan, N. E. Dahlen, and R. van Leeuven, J. Chem. Phys. **130**, 114105 (2009).

[8] M. Rohlfing, P. Krüger, and J. Pollmann, Phys. Rev. B **52**, 1905 (1995).

[9] X. Blase, and P. Ordejón, Phys. Rev. B **69**, 085111 (2004).

[10] D. Foerster, J. Chem. Phys. **128**, 034108 (2008).

[11] D. Foerster, P. Koval, J. Chem. Phys. **131** 044103 (2009).

[12] J. E. Harriman, Phys. Rev. **A 34**, 29 (1986).

[13] H. Koch, A. Sánchez de Merás, and Th. B. Pedersen, J. Chem. Phys. **118**, 9481 (2003).

[14] Th. B. Pedersen, F. Aquilante, and R. Lindh, Theor. Chem. Acc. **124**, 1 (2009).

[15] J. D. Talman, Int. J. Quant. Chem. **107**, 1578 (2007); Comput. Phys. Commun. **30**, 93 (1983); Comput. Phys. Commun. **180**, 332 (2009).

[16] U. Larrue, *Etude de la densité spectrale d'une métrique associée a l'equation de Schrödinger pour l'hydrogene*, unpublished (Bordeaux, 2008). This study showed an asymptotically uniform density of eigenvalues, on a logarithmic scale, for the metric of local products of the hydrogen atom.

[17] R. Brown, private communication (Bordeaux, 2007).

[18] A. L. Fetter, J. D. Walecka, *Quantum Theory of Many-Particle Systems* (McGraw-Hill, New York, 1971).

[19] For convenience, we use time-ordered, rather than causal correlators.

[20] Harrison W. A. *Solid State Theory* (McGraw-Hill, New York, 1970).

[21] P. Ordejón, E. Artacho and J. M. Soler, Phys. Rev. **B 53**, R10441 (1996); J. M. Soler, E. Artacho, J. D. Gale, A. García, J. Junquera, P. Ordejón, D. Sánchez-Portal, J. Phys. **C 14**, 2745 (2002). We used SIESTA version 2.0.1 to perform calculations in this work.

[22] M. Petersilka, U. J. Gossmann, and E. K. U. Gross, Phys. Rev. Lett., **76**, 1212 (1996).

[23] V. I. Lebedev, Russ. Acad. Sci. Dokl. Math. **50**, 283 (1995). http://www.ccl.net/cca/software/SOURCES/FORTRAN/Lebedev-Laikov-Grids/

[24] Y. Saad, *Iterative Methods for Sparse Linear Systems* (Siam, Philadelphia 2003).

[25] P. Giannozzi, S. Baroni, N. Bonini, M. Calandra, R. Car, C. Cavazzoni, D. Ceresoli, G. L. Chiarotti, M. Cococcioni, I. Dabo, A. Dal Corso, S. Fabris, G. Fratesi, S. de Gironcoli, R. Gebauer, U. Gerstmann, C. Gougoussis, A. Kokalj, M. Lazzeri, L. Martin-Samos, N. Marzari, F. Mauri, R. Mazzarello, S. Paolini, A. Pasquarello, L. Paulatto, C. Sbraccia, S. Scandolo, G. Sclauzero, A. P. Seitsonen, A. Smogunov, P. Umari, R. M. Wentzcovitch, J. Phys.: Condens. Matter, **21**, 395502 (2009).

[26] E. E. Koch and A. Otto, Chem. Phys. Lett. **12**, 476 (1972).

[27] R. M. Martin, *Electronic structure: basic theory and practical methods* (Cambridge University Press, 2004).

[28] http://www.icmab.es/siesta/

[29] http://www.abinit.org/

[30] R. Bauernschmitt, R. Ahlrichs, F. H. Hennrich, and M. M. Kappes, J. Am. Chem. Soc. **120**, 5052 (1998).

[31] D. Rocca, R. Gebauer, Y. Saad, and S. Baroni, J. Chem. Phys. **128**, 154105 (2008).

[32] R. Brown, IPREM, unpublished (Pau, 2008).

[33] R. Brown, private communication (Biarritz, 2009).

[34] M. Rohlfing and S. G. Louie, Phys. Rev. Lett. **81**, 2312 (1998); for recent work, see L. Tiago and J. R. Chelikowsky, Phys. Rev. **B 73**, 205334 (2006).

[35] F. Sottile, M. Marsili, V. Olevano, and L. Reining, Phys. Rev. **B 76**, 161103(R) (2007).

[36] L. Hedin, Phys. Rev. **139**, A796–A823 (1965).

[37] M. M. Rieger, L. Steinbeck, I. D. White, H. N. Rojas, R. W. Godby, Comput. Phys. Commun. **117**, 211 (1999).